

Supporting information for

Theoretical prediction and experimental verification of the chemically-ordered atomic-laminate *i*-MAX phases $(\text{Cr}_{2/3}\text{Sc}_{1/3})_2\text{GaC}$ and $(\text{Mn}_{2/3}\text{Sc}_{1/3})_2\text{GaC}$

Andrejs Petruhins*, Martin Dahlqvist, Jun Lu, Lars Hultman, and Johanna Rosen*

Thin Film Physics, Department of Physics, Chemistry and Biology (IFM), Linköping University, SE-581 83, Linköping, Sweden

*Corresponding author. Email: andrejs.petruhins@liu.se, johanna.rosen@liu.se

This file includes:

Tables SI-SVIII

Figures S1-S4

Table SI. Prototype structure, with corresponding structural information, and calculated total energy per formula unit for considered competing phases within present paper.

Phase	Prototype	Pearson symbol	Space group	Energy (eV/fu)
Cr	W	cI2	Im-3m (229)	-9.6430
Cr	Cu	cF4	Fm-3m (225)	-9.2408
Cr	Mg	hP2	P6 ₃ /mmc (194)	-9.2298
Mn	α -Mn	cI58	I-43m (217)	-9.1582
Mn	β -Mn	cP20	P4 ₁ 32 (213)	-9.1056
Mn	AuCu	tP4	P4/mmm (123)	-9.1297
Mn	CsCl	cP2	Pm-3m (221)	-9.0107
Sc	Mg	hP2	P6 ₃ /mmc (194)	-6.3327
Sc	Np	tP4	P4/nmm (129)	-6.2230
Sc	Sc	hP6	P6122 (178)	-6.2006
α -Ga	Ga	oC8	Cmca (64)	-3.0302
Ga	Ga	oC4	Cmcm (63)	-3.0121
Ga	Ga	mC4	C2/c (15)	-3.0119
C	C (graphite)	hP4	P6 ₃ /mmc (194)	-9.2246
Cr_{23}C_6	Cr_{23}C_6	cF116	Fm-3m (225)	-279.3407

Cr ₃ C	Fe ₃ C	oP16	Pnma (62)	-38.4634
Cr ₇ C ₃	Cr ₇ C ₃	oP40	Pnma (62)	-96.2272
Cr ₃ C ₂	Sb ₂ S ₃	oP20	Pnma (62)	-47.9107
Mn ₂₃ C ₆	Cr ₂₃ C ₆	cF116	Fm-3m (225)	-268.6277
Mn ₃ C	Fe ₃ C	oP16	C2/c (15)	-64.7226
Mn ₅ C ₂	Mn ₅ C ₂	mS28	Pnma (62)	-92.4925
Mn ₇ C ₃	Cr ₇ C ₃	oP40	P63mc (186)	-92.4221
MnC	NiAs	hP4	P6 ₃ /mmc (194)	-18.1687
Sc ₂ C	CdI ₂	hP3	P3m1 (156)	-23.2708
Sc ₂ C	Ti ₂ C	cF48	Fd-3m (227)	-23.2657
Sc ₄ C ₃	Th ₃ P ₄	cI28	I-43d (220)	-56.4192
ScC _{0.875}	NaCl	cF8	Fm-3m (225)	-14.9227
ScC	NaCl	cF8	Fm-3m (225)	-15.8395
Sc ₃ C ₄	Sc ₃ C ₄	tP70	P4/mnc (128)	-58.7638
Cr ₃ Ga	Cr ₃ Si (β -W)	cP8	Pm-3n (223)	-32.1352
CrGa	MnGa	hR78	R-3m (166)	-12.7091
Cr ₃ Ga ₄	Fe ₃ Ga ₄	mS42	C12/m1 (12)	-41.2187
CrGa ₄	Hg ₄ Pt	cI10	Im-3m (229)	-22.5270
Mn ₃ Ga	TiAl ₃	tI8	I4/mmm (139)	-30.9155
Mn ₃ Ga	Ni ₃ Sn	hP8	P6 ₃ /mmc (194)	-30.6467
MnGa	AuCu	tP2	P4/mmm (123)	-12.4531
MnGa	CuPt	hR32	R-3m (166)	-12.1692
MnGa	Mg	hP2	P6 ₃ /mmc (194)	-12.2589
MnGa	MnGa	hR78	R-3m (166)	-12.4090
Mn ₅ Ga ₈	Cr ₅ Al ₈	hR26	R3m (160)	-70.6863
Mn ₂ Ga ₅	Mn ₂ Hg ₅	tP14	P4/mmb (127)	-34.3720
MnGa ₄	PtHg ₄	cI10	Im-3m (229)	-22.1774
MnGa ₆	MnAl ₆	oC28	Cmcm (63)	-27.5430
Sc ₅ Ga ₃	Y ₅ Ga ₃	mS32	C12/m1 (12)	-44.9893
Sc ₁₁ Ga ₁₀	Ho ₁₁ Ge ₁₀	tI84	I4/mmm (139)	-112.2262
ScGa	TII	oS8	Cmcm (63)	-9.0837
ScGa ₂	KHg ₂	oI12	Imma (74)	-14.0796
ScGa ₃	AuCu ₃	cP4	Pm-3m (221)	-17.3922
Cr ₃ GaC	CaTiO ₃	cP5	Pm-3m (221)	-41.0458
Cr ₃ GaC	Re ₃ B	oP20	Cmcm (63)	-41.4353
Cr ₂ GaC	Cr ₂ AlC	hP8	P6 ₃ /mmc (194)	-32.0973
Cr ₃ GaC ₂	Ti ₃ SiC ₂	hP12	P6 ₃ /mmc (194)	-50.6991
Cr ₄ GaC ₃	Ti ₄ AlN ₃	hP12	P6 ₃ /mmc (194)	-69.3788
Mn ₃ GaC	CaTiO ₃	cP5	Pm-3m (221)	-40.2921
Mn ₃ GaC	Re ₃ B	oP20	Cmcm (63)	-40.3287
Mn ₃ GaC	Cr ₃ AsN	tI20	I4/mcm (140)	-40.2893
Mn ₂ GaC	Cr ₂ AlC	hP8	P6 ₃ /mmc (194)	-31.1598
Mn ₃ GaC ₂	Ti ₃ SiC ₂	hP12	P6 ₃ /mmc (194)	-49.2157
Mn ₄ GaC ₃	Ti ₄ AlN ₃	hP12	P6 ₃ /mmc (194)	-67.0531
Sc ₃ GaC	CaTiO ₃	cP5	Pm-3m (221)	-34.2348
Sc ₂ GaC	Cr ₂ AlC	hP8	P63/mmc (194)	-27.0471
Sc ₃ GaC ₂	Ti ₃ SiC ₂	hP12	P63/mmc (194)	-43.0551
Sc ₄ GaC ₃	Ti ₄ AlN ₃	hP16	P63/mmc (194)	-58.9402
Sc ₂ CrC ₃	Sc ₂ CrC ₃	oP24	Pbam (55)	-52.4688
β -ScCrC ₂	ScCrC ₂	hP8	P6 ₃ /mmc (194)	-35.8144
Cr ₂ ScGaC ₂	Cr ₂ TiAlC ₂	hP12	P6 ₃ /mmc (194)	-48.4666
Sc ₂ CrGaC ₂	Cr ₂ TiAlC ₂	hP12	P6 ₃ /mmc (194)	-45.8395
CrSc ₂ C	CuHg ₂ Ti	cF16	F-43m (216)	-27.7394

CrSc ₂ C	AlCu ₂ Mn	cF16	Fm-3m (225)	-28.4508
ScMn ₂	MgZn ₂	hP12	P6 ₃ /mmc (194)	-25.0744
MnSc ₂ C	CuHg ₂ Ti	cF16	F-43m (216)	-28.1878
MnSc ₂ C	AlCu ₂ Mn	cF16	Fm-3m (225)	-28.9198
Sc ₃ Mn ₂ Ga ₆	Sc ₃ Mn ₂ Ga ₆	oP44	Pnma (62)	-60.5657

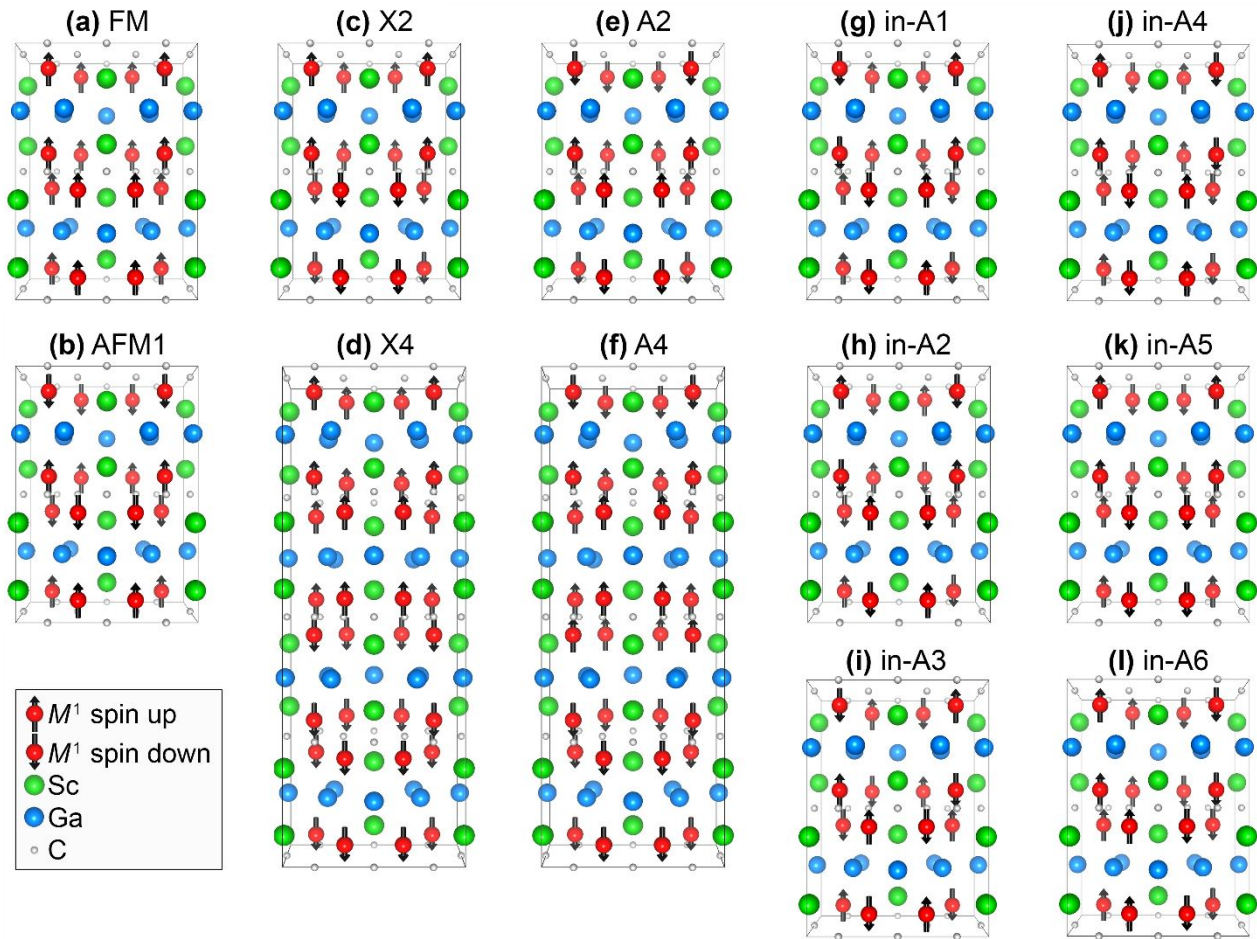


Figure S1. Schematic representation of 12 collinear spin configurations considered for $(M^1_{2/3}Sc_{1/3})_2GaC$, $M^1 = Cr$ or Mn , where the spin direction at each M^1 site is represented by a black arrow.

Table SII. Identified equilibrium simplex and corresponding formation enthalpy for Cr_2GaC , Mn_2GaC and Sc_2GaC phases ($P6_3/mmc$ structure), and the hypothetical i -MAX phases $(\text{Sc}_{2/3}\text{Cr}_{1/3})_2\text{GaC}$ and $(\text{Sc}_{2/3}\text{Mn}_{1/3})_2\text{GaC}$. Please note that the former i -MAX phase diverge from an i -MAX structure upon relaxation, i.e. the phase is not stable for such atom configuration. Relaxation performed using the PBE exchange-correlation functional.

Phase	equilibrium simplex	Spin configuration [†]	ΔH_{cp} (meV/atom)	experimental observation
Cr_2GaC	Cr_3C_2 , CrGa_4 , Cr_7C_3	in-AFM1	-19	yes
Mn_2GaC	Mn_3GaC , C, MnGa_4	AFM[0001] ₄ ^A	-31	yes
Sc_2GaC	Sc_3GaC , ScGa_2 , Sc_3C_4	NM	11	no
$(\text{Sc}_{2/3}\text{Cr}_{1/3})_2\text{GaC}$	$(\text{Cr}_{2/3}\text{Sc}_{1/3})_2\text{GaC}$, ScGa_2 , Sc_3GaC , Sc_2CrC_3	NM	-5	no
$(\text{Sc}_{2/3}\text{Mn}_{1/3})_2\text{GaC}$	$(\text{Mn}_{2/3}\text{Sc}_{1/3})_2\text{GaC}$, Sc_3GaC , ScGa_2 , Sc_3C_4	NM	+12	no

[†] Results attained form Ref. [10] for Cr_2GaC and Ref. [11] for Mn_2GaC .

Table SIII. Calculated energy and corresponding structural and magnetic information for $(\text{Cr}_{2/3}\text{Sc}_{1/3})_2\text{GaC}$ when considering different spin configurations. Relaxation performed using the PBE exchange-correlation functional.

Spin configuration	Space group	a (Å)	b (Å)	c (Å)	Notes	ΔE_{NM} (meV/atom)	magnetic moment (μ_B / Cr atom)
NM	63	9.0569	5.1800	12.7669		0	0.00
FM	63	9.0926	5.2088	12.7481		-0.7	0.73
AFM1			goes to the NM state				
X2	63	9.0708	5.1951	12.7722		-1.7	0.72
A2			goes to the NM state				
X4	12	5.2075	9.0888	12.7550	$\beta=90.0872^\circ$	-1.0	0.79, 0.80
A4	38	12.7541	9.0600	5.1864	mix of A2 and AFM1	-0.7	0.48, 0.61
in-AFM1			goes to the NM state				
in-AFM2			goes to the NM state				
in-AFM3			goes to the NM state				
in-AFM4			goes to the NM state				
in-AFM5			goes to the NM state				
in-AFM6	63	9.0791	5.1957	12.7547		-2.7	0.63

Table SIV. Calculated energy and corresponding structural and magnetic information for $(\text{Mn}_{2/3}\text{Sc}_{1/3})_2\text{GaC}$ when considering different spin configurations. Relaxation performed using the PBE exchange-correlation functional.

Spin configuration	Space group	a (Å)	b (Å)	c (Å)	Notes	ΔE_{NM} (meV/atom)	magnetic moment ($\mu_B / \text{Mn atom}$)
NM	63	8.9901	5.1385	12.5482		0	0.00
FM					goes to the NM state		
AFM1	63	8.9900	5.1419	12.5850		-1.1	0.72
X2					goes to the NM state		
A2					goes to the NM state		
X4	12	5.1397	8.9914	12.5611	$\beta=90.0032^\circ$ mix of A2 and AFM1	-0.2	0.24, 0.50
A4					goes to the NM state		
in-AFM1					goes to the NM state		
in-AFM2					goes to the NM state		
in-AFM3					goes to the NM state		
in-AFM4					goes to the NM state		
in-AFM5					goes to the NM state		
in-AFM6					goes to the NM state		

Table SV. Calculated energy and corresponding structural and magnetic information for $(\text{Cr}_{2/3}\text{Sc}_{1/3})_2\text{GaC}$ when considering different spin configurations. Relaxation performed using the PBE exchange-correlation functional with +U method, where $U_{\text{eff}} = 1 \text{ eV}$.

Spin configuration	Space group	a (Å)	b (Å)	c (Å)	Notes	ΔE_{NM} (meV/atom)	magnetic moment ($\mu_B / \text{Cr atom}$)
NM	63	9.0533	5.1824	12.7838		0	0.00
FM	63	9.0995	5.2364	12.8101		-24	1.29
AFM1	63	9.1256	5.2570	12.8569		-23	1.57
X2	63	9.1169	5.2460	12.8462		-31	1.56
A2	63	9.1105	5.2521	12.8189		-22	1.37
X4	12	5.2422	9.1015	12.8323	$\beta=90.0220^\circ$	-28	1.30, 1.54
A4	38	12.8135	9.1030	5.2444		-24	1.29, 1.36
in-AFM1	63	9.0833	5.1917	12.7655		-1.5	0.55
in-AFM2	63	9.0572	5.1995	12.7896		-0.6	0.54
in-AFM3					goes to the NM state		
in-AFM4	63	9.0748	5.2260	12.7770		-5.7	1.00
in-AFM5	63	9.0598	5.2282	12.8228		-29	1.06
in-AFM6	63	9.1202	5.2123	12.7778		-29	1.06

Table SVI. Calculated energy and corresponding structural and magnetic information for $(\text{Mn}_{2/3}\text{Sc}_{1/3})_2\text{GaC}$ when considering different spin configurations. Relaxation performed using the PBE exchange-correlation functional with +U method, where $U_{\text{eff}} = 1 \text{ eV}$.

Spin configuration	Space group	a (Å)	b (Å)	c (Å)	Notes	ΔE_{NM} (meV/atom)	magnetic moment (μ_B / Mn atom)
NM	63	8.9848	5.1348	12.5553		0	0.00
FM	63	9.1086	5.2834	12.7238		-25	2.16
AFM1	63	9.0510	5.1932	12.7282		-39	1.90
X2	63	9.0618	5.2280	12.7330		-31	2.07
A2	63	9.1072	5.2792	12.6762		-26	2.31
X4	12	5.2438	9.0707	12.6985	90.2385	-28	2.05, 2.21
A4	38	12.6983	9.1109	5.2807		-26	2.34, 2.40
in-AFM1	63	9.0407	5.1684	12.6277		-4.2	1.27
in-AFM2	63	8.9809	5.2704	12.8601		-25	2.24
in-AFM3	63	9.1208	5.1892	12.7721		-22	2.10
in-AFM4	63	8.9605	5.2779	12.8983		-2.8	2.29
in-AFM5	63	9.0087	5.2494	12.7079		-15	1.92
in-AFM6	63	9.0231	5.2354	12.6943		-16	1.84

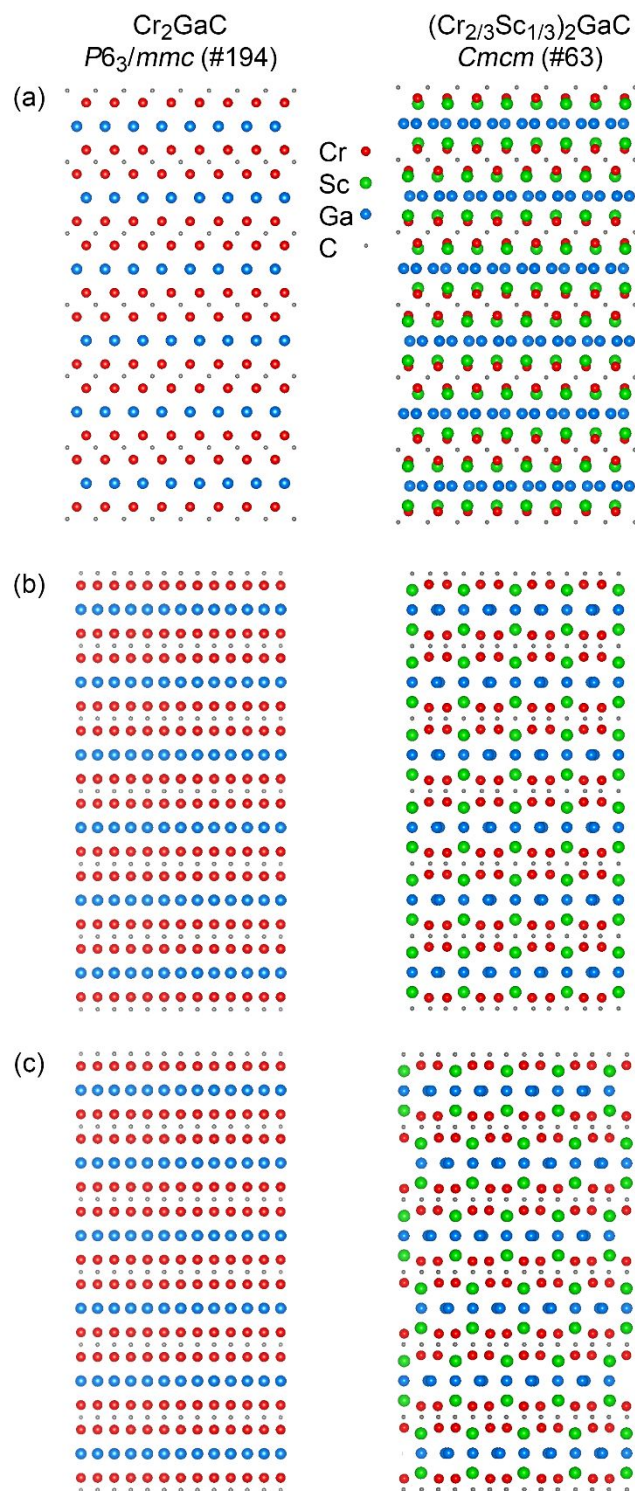


Figure S2. Schematic representation of the Cr_2GaC MAX phase and $(\text{Cr}_{2/3}\text{Sc}_{1/3})_2\text{GaC}$ *i*-MAX phase when viewed along a) [100], b) [010] and c) [110] zone axis. The primary structural difference between the MAX phase and the *i*-MAX phase is the in-plane chemical order within the *M*-layer,

to allow formation of a honeycomb pattern where the larger elements approach the A-layer. The A-layer, in turn, change its structure into Kagomé-like ordering, altogether resulting in an orthorhombic crystal structure of space group *Cmcm* for the herein reported phases. Based on previously reported theoretical analysis of structure, bonding, and related stability, we suggest that the formation of *i*-MAX is favored for increasing size difference between the two metals, and with decreasing size of the A-element.

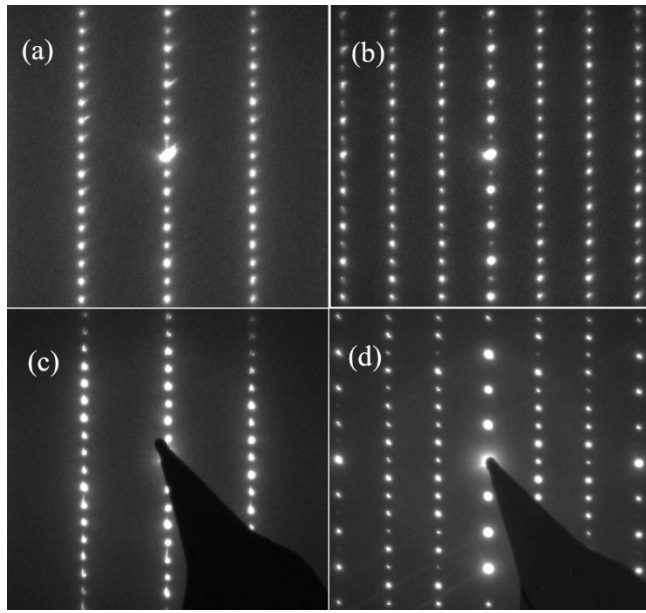


Figure S3. Selected area electron diffraction (SAED) of $(\text{Cr}_{2/3}\text{Sc}_{1/3})_2\text{GaC}$ along the [100] (a) and [110] (b) zone axis, and of $(\text{Mn}_{2/3}\text{Sc}_{1/3})_2\text{GaC}$ along the [100] (c) and [110] (d) zone axis.

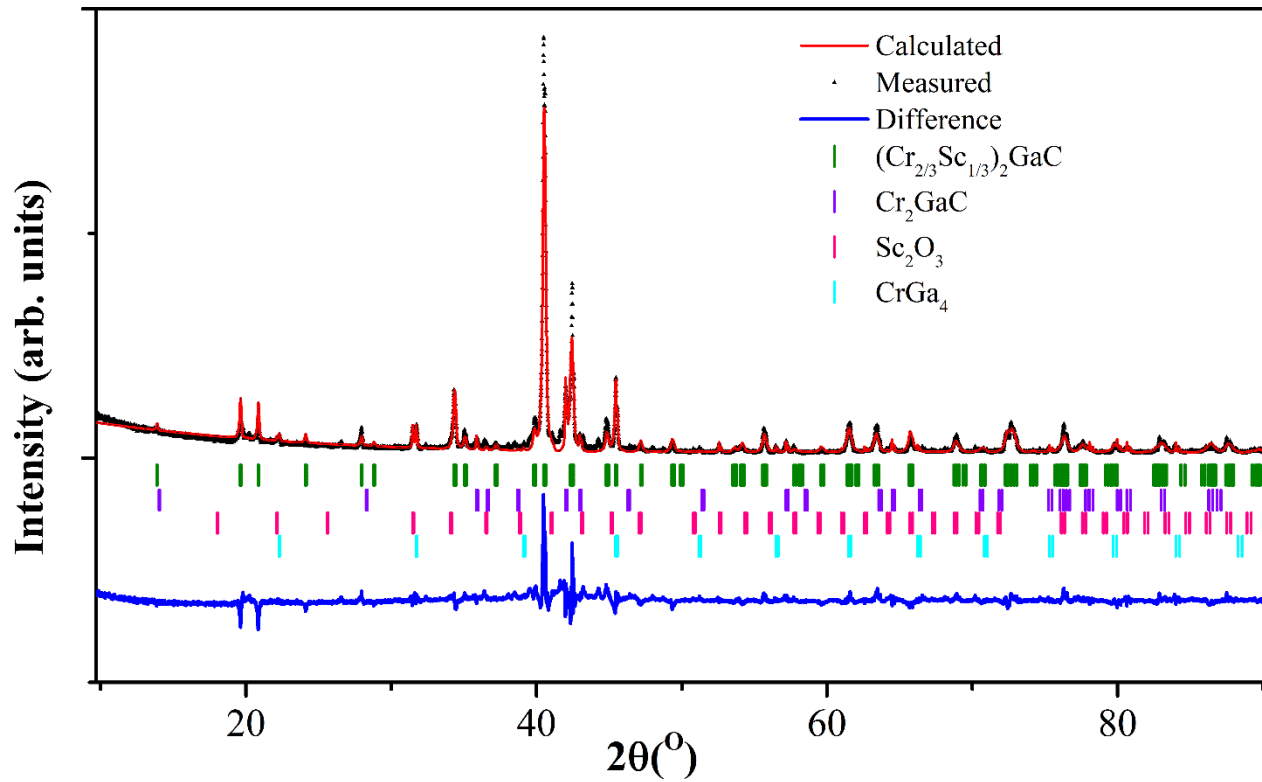


Figure S4. Rietveld refinement of XRD data for the $(\text{Cr}_{2/3}\text{Sc}_{1/3})_2\text{GaC}$ sample.

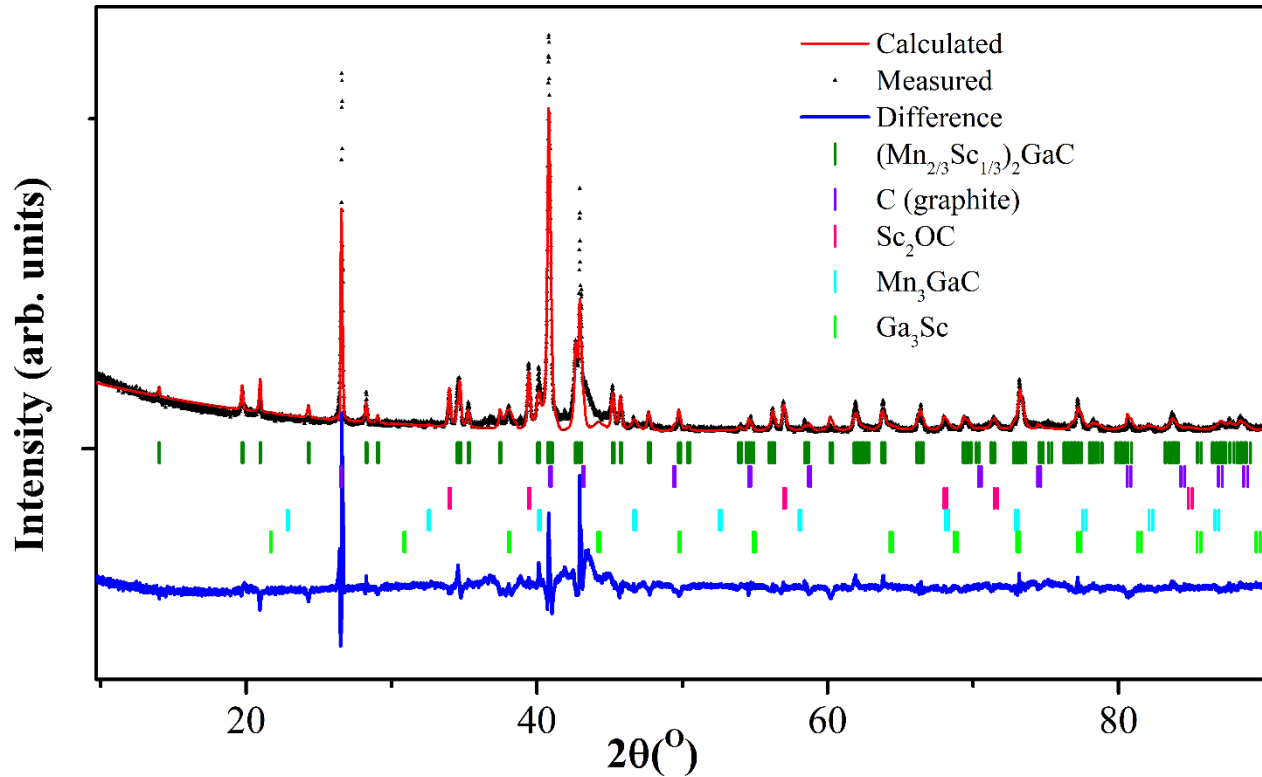


Figure S5. Rietveld refinement of XRD data for the $(\text{Mn}_{2/3}\text{Sc}_{1/3})_2\text{GaC}$ sample.

Table SVII. Cell parameters and atom coordinates obtained from XRD Rietveld refinement at RT. Upon attempted change in occupancy (from 1.0) as well as Cr/Mn intermixing, there was no improvement in the refinement.

Space group	<i>Cmcm</i> (#63)	<i>Cmcm</i> (#63)
System	Cr-Sc-Ga-C	Mn-Sc-Ga-C
χ^2	13.0	10.1
a (Å)	9.05649(34)	8.99827(60)
b (Å)	5.21497(20)	5.19006(36)
c (Å)	12.76932(40)	12.62758(46)
	$\alpha = \beta = \gamma = 90^\circ$	
<i>M</i> ¹	Cr, 16h 0.8364(2) 0.3269(17) 0.5771(3)	Mn, 16h 0.8364(14) 0.3251(30) 0.5761(4)
Sc	8f 0.0000 0.1671(23) 0.3914(5)	8f 0.0000 0.1815(31) 0.3910(5)
Ga	4c 0.0000 0.6799(16) 0.2500 8g 0.7655(5) 0.4071(11) 0.2500	4c 0.0000 0.6762(18) 0.2500 8g 0.76362(9) 0.43975(13) 0.2500
C	8e 0.8410(30) 0.0000 0.0000 4b 0.0000 0.5000 0.0000	8e 0.8590(32) 0.0000 0.0000 4b 0.0000 0.5000 0.0000

Table SVIII. Phase purity obtained from Rietveld refinement in wt.%

System	Composition				
Cr-Sc-Ga-C	(Cr _{2/3} Sc _{1/3}) ₂ GaC 86.8%	Cr ₂ GaC 6.1%	Sc ₂ O ₃ 4.1%	CrGa ₄ 3.0%	
Mn-Sc-Ga-C	(Mn _{2/3} Sc _{1/3}) ₂ GaC 61.4%	C (graphite) 25.1%	Sc ₂ OC 6.8%	Mn ₃ GaC 3.2%	Ga ₃ Sc 3.5%